CONF-880793--1

CONF-880793--1

DE88 015299

Poloidal VV Currents, Disruption-Induced VV Forces, and TSC-EIGENCIRC Interfaces

R. O. Sayer
Fusion Engineering Design Center
Oak Ridge National Laboratory

CIT PF Workshop - PPPL

July 12, 1988

- Poloidal VV currents induced by toroidal flux changes.
- TSC Disruption-Induced Forces on the CIT 2.10 m Vacuum Vessel
- Status of EIGENCIRC-TSC Interface.
- TSC Disruption Run with External TF Structure

*RESEARCH SPONSORED BY THE OFFICE OF FUSION ENERGY, U.S. DEPARTMENT OF ENERGY, UNDER CONTRACT DE-AC05-84OR21400 WITH MARTIN MARIETTA ENERGY SYSTEMS, INCORPORATED.

Forces due to poloidal VV currents

TSC computes VV forces arising from toroidal currents due to poloidal flux changes; forces due to toroidal flux changes are not calculated explicitly. However, one source of induced VV poloidal current may be estimated from the TSC plasma paramagnetism, namely the difference between the toroidal field and the vacuum field, integrated over the plasma volume. This "paramagnetic" flux, Φ_{para} is used in a simple circuit equation to determine the poloidal VV current, I_{vvpol} . The corresponding force histories are calculated in the post-processor code, TWIR.

Circuit Equation

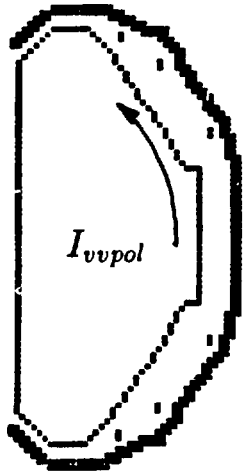

Consider the VV as a loop with current I_{vvpol} flowing in the poloidal direction as a result of change in toroidal flux throughout the plasma volume. Neglect mutual inductances between the VV and plasma and between the VV and surrounding structures. The circuit equation is

$$L_{vv}\, dI_{vvpol}/dt + R_{vv}\, I_{vvpol} = -d\Phi_{para}/dt \qquad (1)$$

where L_{vv} is the VV self inductance and R_{vv} is the resistance to poloidal current flow. The resistance is

$$R_{vv} = \rho * (165"wires" * 0.05m)/A = 15.6x10^{-6}\Omega \qquad (2)$$

A code written by S. Kalsi was used to compute $L_{vv} = 0.411\mu H$ for the 2.10 m VV geometry. As a check, the self inductance of a rectangular toroid of size approximating the VV was calculated to be $0.29\mu H$.

The circuit equation (1) is solved in TSC using Φ_{para} (=DIAMAG) and integrating forward in time:

$$I_{vvpol}(n) = (\Phi_{para}(n-1) - \Phi_{para}(n) + L_{vv} * I_{vvpol}(n-1)) \\ /(L_{vv} + R_{vv} * (t_n - t_{n-1}) \quad (3)$$

For a major disruption of the type considered here, Φ_{para} increases from a small value to a large positive value during the 0.2 ms thermal quench. For example, for FBCHIA = 20000, dI_p/dt = - 3.4 MA/ms, Φ_{para} increases from -0.25 to 0.53 webers in about 0.2 ms. Over this time scale the solution is inductive and the maximum current is approximately

$$I_{vvpol} \simeq 0.78 webers/0.411\mu H = 1.9MA \quad (4)$$

The actual maximum current from equation (3) is 1.82 MA. As the current quench proceeds, Φ_{para} decreases slowly to zero, and I_{vvpol} decays with a time constant of $L_{vv}/R_{vv} = 0.411/15.6 = 26.3ms$.

Let F_{vvpol}(i) be the force in Nt/rad on an element of length dl, and let $G_o = R * B_t$, where B_t is the vacuum toroidal field. Then

$$F_{vvpol}(i) = I_{vvpol}\, dl\, G_o/(2\pi\, R_i) \quad (5)$$

where R_i is the radius of the element i.

CITPFW3 R. O. Sayer 12 July 1988

Examples

The following figures show force distributions from: a) toroidal VV currents only, b) poloidal VV currents only, c) toroidal VV currents AND poloidal VV currents , and d) $F_r(net)$ vs. time.

1. Snapshot of VV force distribution for a vertical disruption case at a time during the thermal quench.
2. Snapshot of VV force distribution for a vertical disruption case at a time about halfway through the current quench.

Observations

- The net vertical force due to poloidal VV currents is zero.
- Net radial forces due to induced poloidal and toroidal VV currents are opposite in sign.
- poloidal VV currents peak soon after the end of the thermal quench.
- The forces due to poloidal VV currents are compressive, yielding a maximum inward pressure of 2.8 MPa for the 3.4 MA/ms case.
- Let $F_{Rnet}(pol)$ and $F_{Rnet}(tor)$ be the net radial VV forces due to poloidal and toroidal currents, respectively. Just after the thermal quench, at the time of extreme $F_{Rnet}(pol)$, we find

$$F_{Rnet}(pol) = -0.60 * F_{Rnet}(tor) \qquad (6)$$

As expected, the result (6) is nearly independent of dI_p/dt since the induced currents at this time are determined almost entirely by geometry.

1. So: poloidal VV currents act to mitigate the net inward VV forces due to toroidal VV currents . Resultant $F_r(net)$ is still inward.
2. But: poloidal VV currents increase the maximum inboard forces by a factor of about two.

TSC Disruption-Induced Forces on the CIT 2.10 m Vacuum Vessel

Model

- The 2.10 m VV was represented by a series of 164 passive filamentary wires based on the geometry of CIT-E-IWB101 (25 Apr 88). The VV material was taken as 5 cm thick Inconel with a resistivity of $1.25 * 10^{-6}\Omega - m$. A modified version of PASSIN (W. Reiersen) was used to generate the TSC "wires". Each wire was moved to the nearest grid point on a 5 x 5 cm mesh.

- The 2.10 m TF support structure was also represented by passive filamentary wires based on the geometry of CIT.WR-10T.MKB.LAYOUT3 (24 Mar 88). The TF structure was assumned to be composed of 10 cm thick SS.

- Each internal coil was represented by two adjacent wires above and two adjacent wires below the midplane.

- Eight external PF coils were used; the TSC circuit equations permitted currents to be induced in external coils. Initial PF coil currents were determined for each set of equilibrium conditions $(R_o, a, \beta_{pol}, \kappa)$ with the ORNL FEDC equilibrium code (D. J. Strickler).

- Vertical Disruptions. An initial displacement was introduced by turning on opposing currents in upper and lower members of internal coil IC1. An equilibrium was obtained with the magnetic axis 9 cm below the midplane. The plasma was then transported for 169 ms until the edge q dropped to 2.1 and the magnetic axis was 45 cm below midplane. The disruption was then initiated by enhancing the thermal conductivity by a factor of 500 to 20000.

Results

Plasma disruption calculations for the CIT 2.10 m, 11.0 MA baseline design have been performed with the Tokamak Simulation Code (TSC) for inward and vertically moving plasmas for Troyon (4.9%) β values for cases corresponding to average current decay rates ranging from 0.25 MA/ms to 3.4 MA/ms.

- Table I gives the initial plasma parameters and coil configuration.
- Table II is a summary of extreme net VV forces for several disruption scenarios.
- Figure 3 contains the magnetic axis trajectory for a vertical disruption and the VV force distribution at a time about halfway through the current quench.
- Figure 4 illustrates the time behavior of net radial and vertical VV forces for a 3.4 MA/ms disruption over the current quench time.
- A vertical disruption run (0614A) with dI_p/dt= -0.25 MA/ms gave the same extreme net vertical force as the 0516D case with dI_p/dt= -0.35 MA/ms.
- The current set of "reference" disruption cases for VV structural analyses is identified as the cases 0623D, 0627A, and 0516D from Table II.

Status of EIGENCIRC-TSC Interfaces.

EC ≡ EIGENCIRC - represents a group of codes by R. Pillsbury for solenoid design and solution of the eigenvalue problem

$$[L]\{dI/dt\} + [R]\{I\} = \{V\} \tag{7}$$

for specified inductance, resistance matrices [L], [R] and specified driving voltages { V} and initial conditions for the current vectors { I} .

Objectives

1. Develop a common electromagnetic model code for representation of PF coils and conducting tokamak structures for input elements of the codes TSC, EC, etc.
   - Well-defined correspondence in geometry and resistance for TSC and EC input elements.
   - Further streamline procedure for generation of input (improve PASSIN).
   - Automatic generation of TSC type 9, 39, 15 cards from EC coil locations sizes, and currents.
2. EC - initial eddy currents in external TF structure for TSC startup runs.
3. Include an EC module in TSC to speed up post-disruption calculations of structural response over long times (seconds).

Figure 5. EC-TSC Interface Chart

Done

- EIGTSC - reads EC output file of external coil locations and sizes and writes TSC type 9, 39 cards for external coils.

- ETEM
  - reads TSC "wire" file and EC output file "EIGOUT".
  - plots TSC wires, EC coils and wires.
  - plots overlay of TSC and EC elements.
  - Figure 6. Overlay of EC MOD061688 and TSC elements.

To Do

- Add currents to EIGTSC.
- Add VV and inner TF structure plots to ETEM.
- Write a code VTW to generate TSC and EC wires such that one EC wire is N x M TSC wires, where N and M are integers. Graphical selection ?
- Scheme for numbering TSC and EC coils, wires, coil groups.
- Specification of number of turns per coil.

TSC Disruption Run with External TF Structure

- Repeat 0623D - inward disruption, $dI_p/dt = 3.0$ MA/ms, with external TF and PF coil casings corresponding to R. Pillsbury's MOD061688.
- EIGTSC: read MOD061688 file and generated TSC type 9, 39 cards.
- TSC dimensions changed to allow additional external coil groups. For the symmetric case run, there were a total of 85 coil groups.
- Inclusion of external TF structure doubles TSC CPU time.
- Inclusion of external TF structure changes the net radial VV force by only 1.3 % .

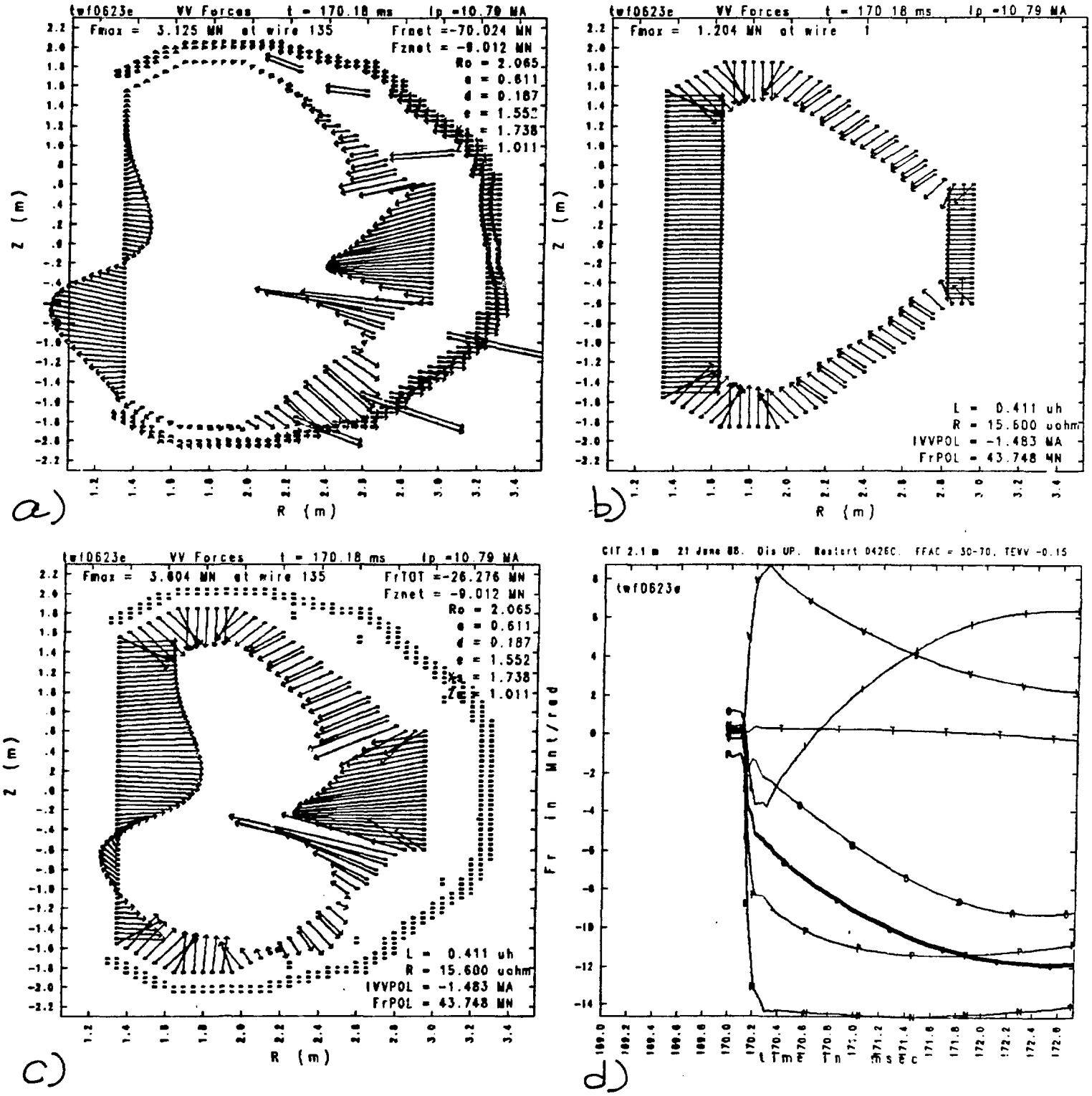

Figure 1. Snapshot of VV force distribution for a vertical disruption during the thermal quench. a) toroidal VV currents only, b) poloidal VV currents only, c) toroidal VV currents AND poloidal VV currents , d) $F_r(net)$ vs. time.

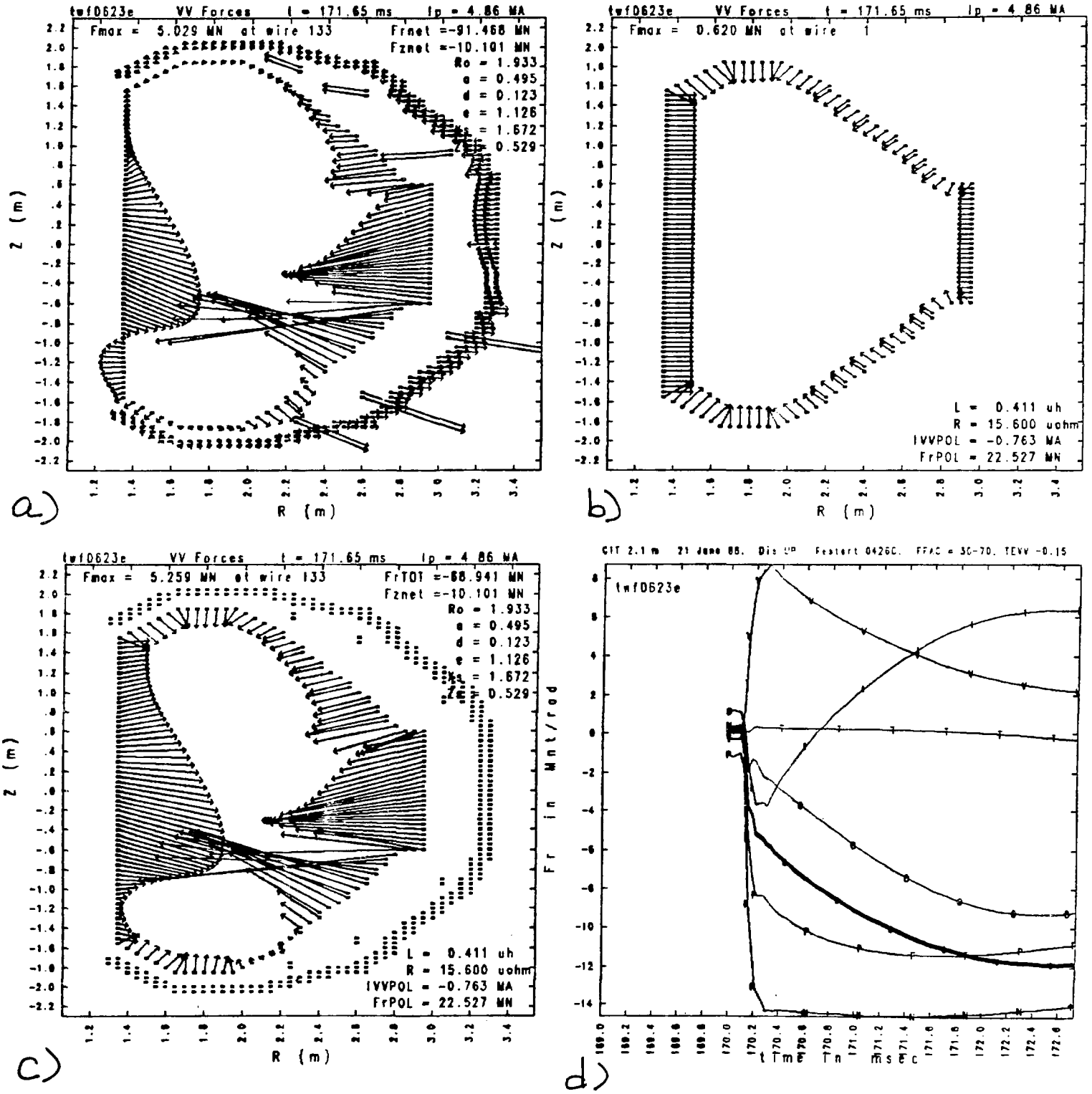

Figure 2. Snapshot of VV force distribution for a vertical disruption about halfway through the current quench. a) toroidal VV currents only, b) poloidal VV currents only, c) toroidal VV currents AND poloidal VV currents , d) $F_r(net)$ vs. time.

CIT 2.1 m VV force distribution at $I_p = 4.86MA$.

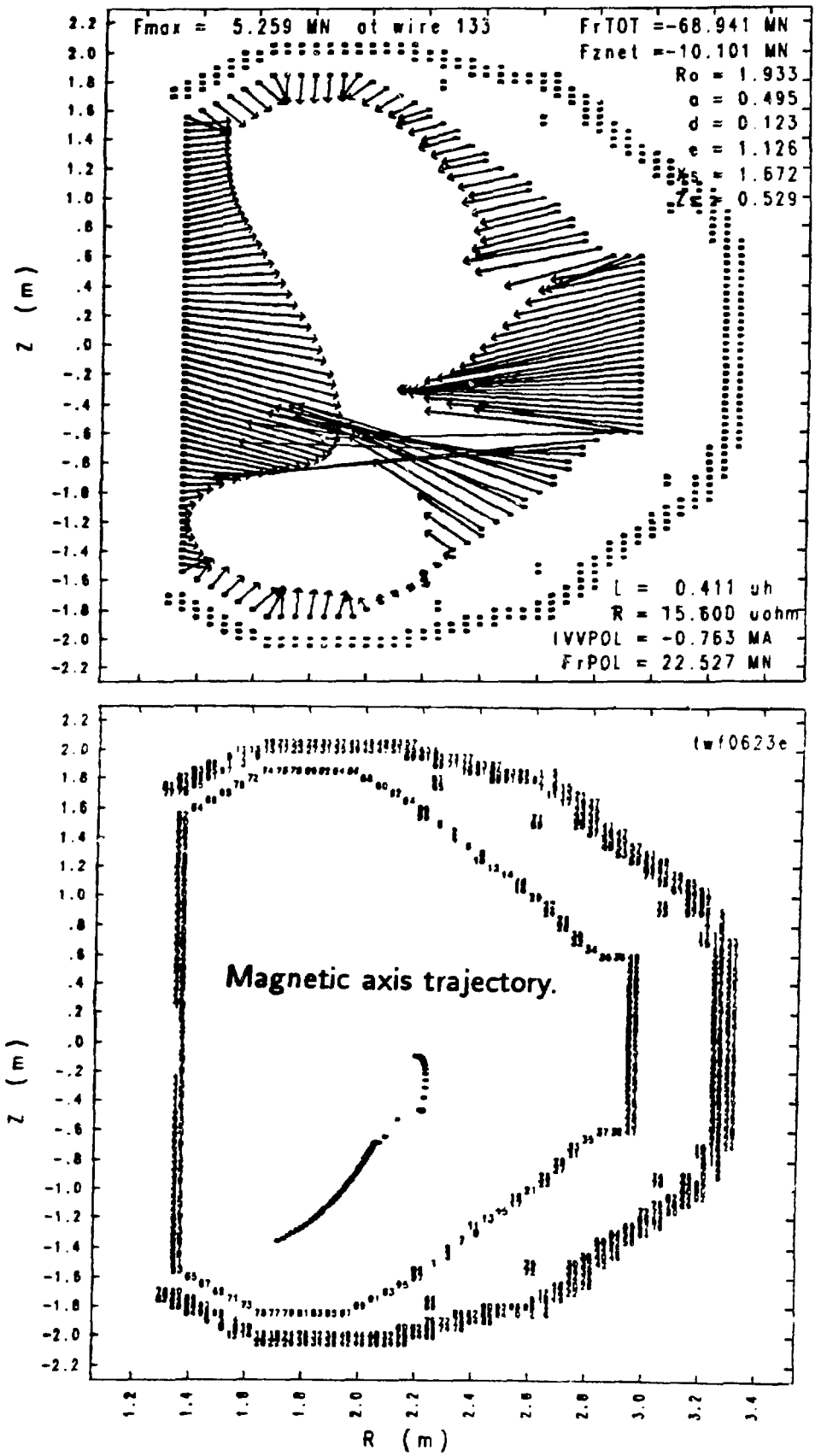

Figure 13

CIT 2.1 m Vacuum Vessel Forces vs. time. $dI_p/dt = -3.4MA/ms.$

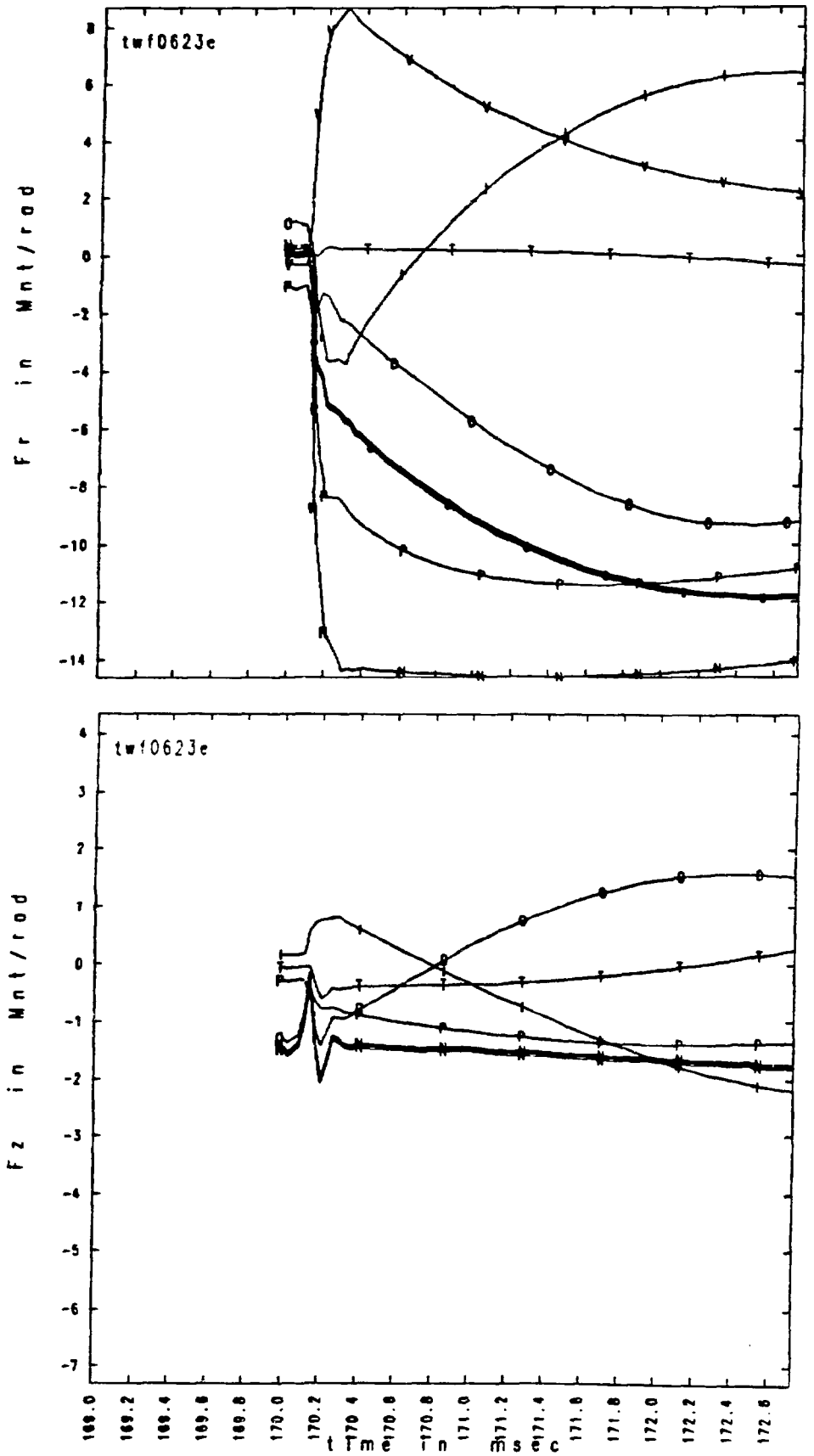

Figure 4

10 JULY 88
ROS

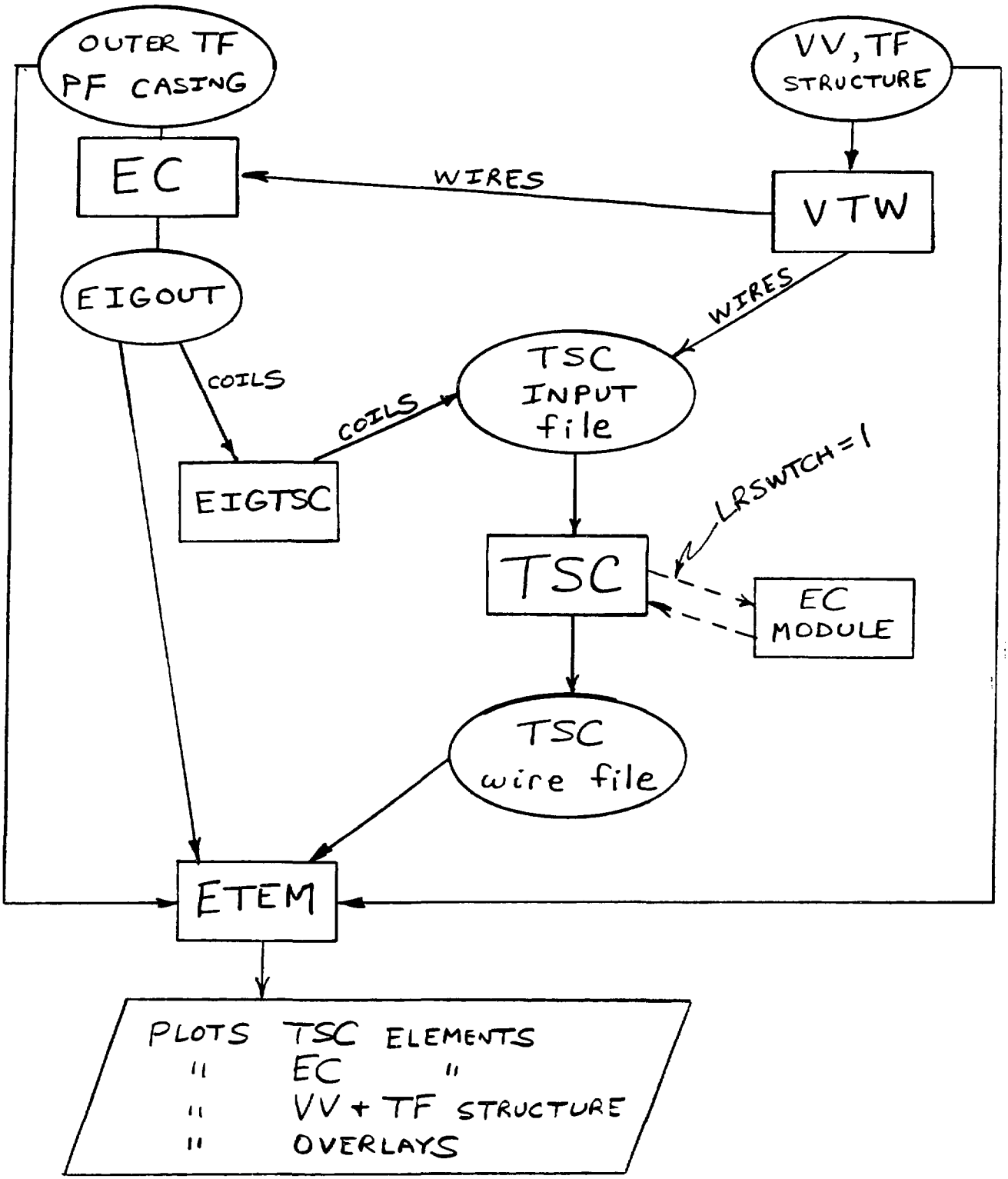

"WIRE" ≡ ELEMENT INTERNAL TO TSC GRID
"COIL" ≡ " EXTERNAL " " "

Figure 5. EC-TSC Interface Chart

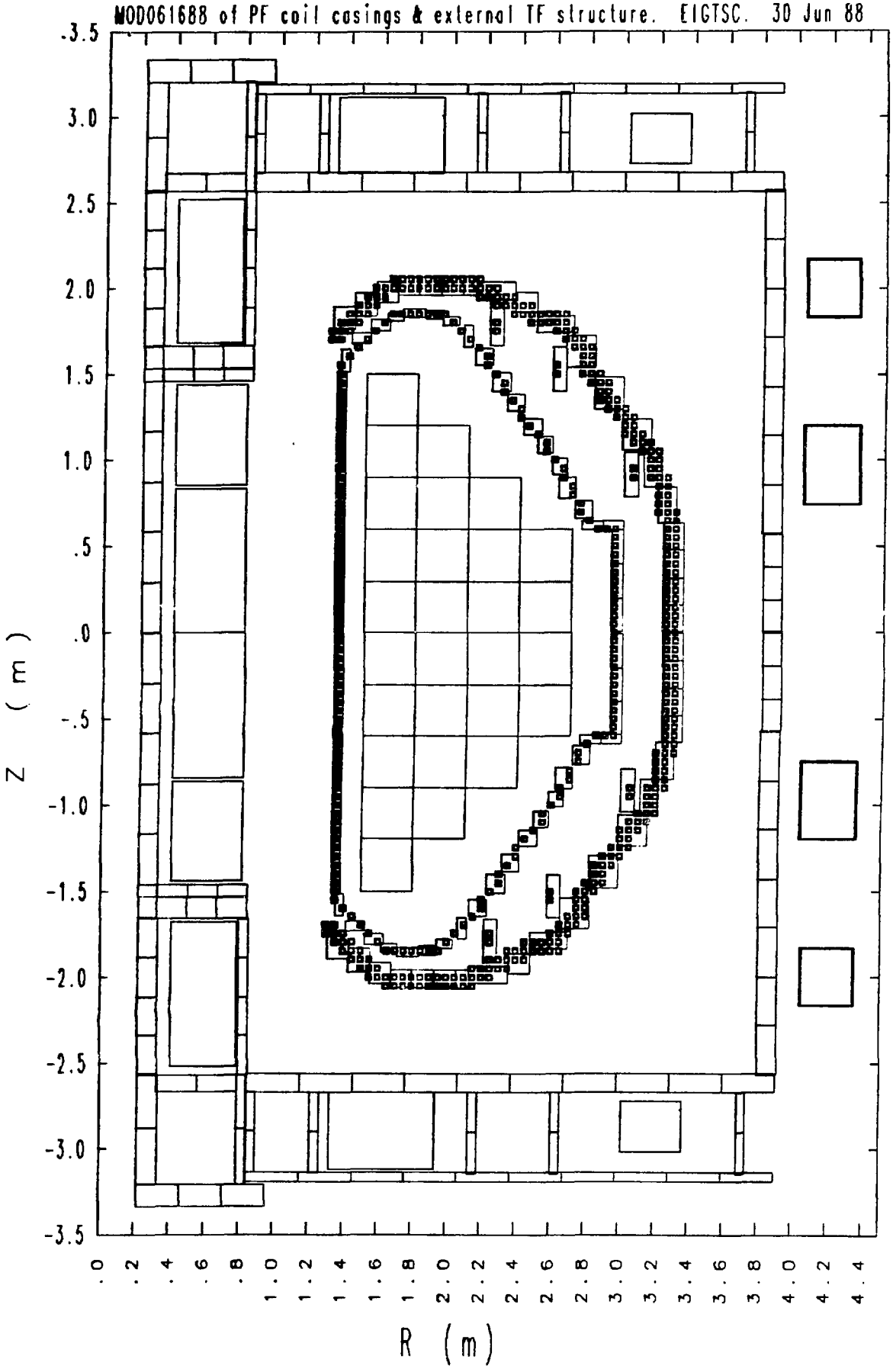

Figure 6. Overlay of EC MOD061688 and TSC elements.

Table I

CIT 2.10 m TSC Disruption Simulations

Initial Plasma Parameters and Coil Configuration

Coil	R(m)	Z(m)	I(MA)
PF1	0.6104	0.0678	-2.553
PF1	0.6104	0.2035	-2.553
PF1	0.6104	0.3392	-2.553
PF1	0.6104	0.4748	-2.553
PF1	0.6104	0.6105	-2.553
PF1	0.6104	0.7462	-2.553
PF2	0.6104	0.8728	1.055
PF2	0.6104	0.9904	1.055
PF2	0.6104	1.1080	1.055
PF2	0.6104	1.2256	1.055
PF2	0.6104	1.3432	1.055
PF3	0.5579	1.7018	0.351
PF3	0.5579	1.8375	0.351
PF3	0.5579	1.9732	0.351
PF3	0.5579	2.1098	0.351
PF3	0.5579	2.2445	0.351
PF3	0.5579	2.3802	0.351
PF4	1.6600	2.8700	4.262
PF5	3.1900	2.8700	0.152
PF6	4.1900	2.0000	-0.823
PF7	4.1900	1.4000	0.0
PF8	4.1900	0.9500	-5.369
IC1	2.2500	1.7500	
IC1	2.2500	1.8000	
IC2	2.6000	1.5000	
IC2	2.6000	1.5500	
IC3	3.0500	0.9000	
IC3	3.0500	0.9500	

Ro(m)	a(m)	Xmag(m)
2.10	0.646	2.19

Ip(MA)	Bt(T)
11.0	10.0

\TIN\PPPL88\JUNVVTAB R. O. Sayer 27 June 1988

Table II

TSC Disruption-Induced CIT 2.1 m Vacuum Vessel Forces

ID	Ip (MA)	dIp/dt (MA/ms)	Zmag (cm)	beta (%)	betapol	Extreme Net Radial Force (MNt/radian)	
0406B	11.0	- 3.0	0	4.9	0.83	-13.32	
0623D	11.0	- 3.0	0	4.9	0.83	-11.15	-11.30 **
0406C	11.0	- 1.1	0	4.9	0.83	-10.22	
0501B	11.0	- 3.4	-45	4.9	0.93	-18.57	-11.72 **
0627A	11.0	- 3.4	-45	4.9	0.93	-14.60	-11.86 **
0503D	11.0	- 0.6	-45	4.9	0.93	-13.46	-7.66 **
0516D	11.0	- 0.35	-45	4.9	0.93	-12.86	-6.15 **

ID	Ip (MA)	dIp/dt (MA/ms)	Zmag (cm)	beta (%)	betapol	Extreme Net Vertical Force (MNt/radian)
0501B	11.0	- 3.4	-45	4.9	0.93	-2.41
0627A	11.0	- 3.4	-45	4.9	0.93	-2.03
0503D	11.0	- 0.6	-45	4.9	0.93	-2.74
0516D	11.0	- 0.35	-45	4.9	0.93	-2.92
0614A	11.0	- 0.25	-45	4.9	0.93	-2.92

** Includes both Jtor x Bpol and Jpol x Btor forces.

The "reference" disruption cases for VV structural analysis are identified as 0623D, 0627A, and 0516D.